Lawrence Berkeley National Laboratory
Lawrence Berkeley National Laboratory

Title
Photovoltaic performance of ultra-small PbSe quantum dots

Permalink
https://escholarship.org/uc/item/2k52x3h3

Author
Ma, Wanli

Publication Date
2011-09-22

Photovoltaic performance of ultra-small PbSe quantum dots

Wanli Ma,[1] Sarah L. Swisher,[2] Trevor Ewers,[1] Jesse Engel,[3] Vivian E. Ferry,[4] Harry A. Atwater,[4] and A. Paul Alivisatos*[1,5]

[1] Department of Chemistry, University of California, Berkeley, California

[2] Department of Electrical Engineering, University of California, Berkeley, California

[3] Department of Materials Science and Engineering, University of California, Berkeley, California

[4] Thomas J. Watson Laboratories of Applied Physics, California Institute of Technology, Pasadena, California

[5] Lawrence Berkeley National Laboratory, Berkeley, California

* To whom correspondence should be addressed. Email: alivis@berkeley.edu

We investigated the effect of PbSe quantum dot size on the performance of Schottky solar cells made in an ITO/PEDOT/PbSe/Aluminum structure, varying the PbSe nanoparticle diameter from 1-3nm. In this highly confined regime, we find that the larger

1

particle bandgap can lead to higher open-circuit voltages (~0.6 V), and thus an increase in overall efficiency compared to previously reported devices of this structure. To carry out this study, we modified existing synthesis methods to obtain ultra-small PbSe nanocrystals with diameters as small as 1 nm, where the nanocrystal size is controlled by adjusting the growth temperature. As expected, we find that photocurrent decreases with size due to reduced absorption and increased recombination, but we also find that the open-circuit voltage begins to decrease for particles with diameters smaller than 2 nm, most likely due to reduced collection efficiency. Due to this effect, we find peak performance for devices made with PbSe dots with a first exciton energy of ~1.6 eV (2.3 nm diameter), with a typical efficiency of 3.5% and a champion device efficiency of 4.57%. Comparing the external quantum efficiency of our devices to an optical model reveals that the photocurrent is also strongly affected by the coherent interference in the thin film due to Fabry-Pérot cavity modes within the PbSe layer. Our results demonstrate that even in this simple device architecture, fine-tuning of the nanoparticle size can lead to substantial improvements in efficiency.

Keywords: PbSe, quantum dot, solar cell, photovoltaic, quantum size effect

---

Over the past four years, lead chalcogenide nanoparticles have been increasingly investigated as a candidate for low-cost, solution-processed photovoltaics.[1] Lead chalcogenides possess an extremely large bulk exciton Bohr radius (46 nm for PbSe and 20 nm for PbS[2]), which creates strong quantum confinement in colloidal nanocrystals and allows their bandgap and absorption edge to be tuned across the entire visible

2

spectrum.[3, 4] Fabrication of Schottky junction solar cells is straightforward with lead chalcogenide quantum dots (QDs): QDs deposited onto indium tin oxide (ITO) form an ohmic contact, and thermally evaporating metal electrodes form the Schottky junction.[5, 6] Early devices made with this structure typically resulted in a solar power conversion efficiency ranging from 1-2%, but would lose nearly all rectification after just minutes of air exposure due to oxidative doping.[5-8] Smaller PbS nanoparticles (<3 nm diameter) were found to overcome this extreme air sensitivity by forming different surface oxidation products due to their reduced faceting.[9] Recently, small PbS dots have been employed in more complex depleted heterojunction solar cell architectures. Photovoltaic devices with efficiencies reaching 5.1% have been achieved for PbS/TiO_2 nanocrystal devices,[10] and PbS/ZnO devices have demonstrated excellent stability for 1000 hours of continuous illumination in ambient air conditions.[11] These demonstrations of improved efficiency and stability motivate the further study of strongly confined quantum dots.

The power conversion efficiency of Schottky solar cells using PbSe quantum dots has typically been limited by low open-circuit voltages (<0.3 V),[5] due in part to the relatively small bandgap of the PbSe quantum dots. In equivalent cells, PbS nanoparticles have demonstrated higher open-circuit voltages than PbSe, but lower photocurrents.[6] PbSe devices tend to have higher photocurrent than PbS, most likely due to the 10-fold increase in the mobility.[12] Using a $PbSe_xS_{1-x}$ alloy proved to be one successful method to combine the best aspects of both materials, improving the open circuit voltage (V_{OC}) from 230 mV to 450 mV while maintaining a short-circuit current (J_{SC}) of 14.8 mA/cm^2.[13] Similar performance (V_{OC} = 440 mV) was achieved by incorporating PbSe QDs into an excitonic solar cell structure,[14] which could theoretically eliminate the

3

constraints on V_{OC} that are inherently imposed by the Schottky architecture. It has also been found that using smaller PbSe QDs with larger bandgaps (E_G) results in a higher V_{OC} in Schottky cells.[5] The improvement scales linearly as $\Delta V_{OC} \propto \Delta E_G/2$, as expected for a Schottky barrier with the Fermi level pinned near the middle of the bandgap. The smallest PbSe QDs in that study were ~3 nm in diameter (E_G = 1.1 eV), which produced a device with V_{OC} = 250 mV. While many recent studies of colloidal lead chalcogenide nanocrystals have focused on carrier multiplication (CM) as a pathway to improving the efficiency of nanocrystal solar cells, a recent perspective on the experimental and theoretical work on CM indicates that the main promise of quantum confinement in colloidal nanocrystals is, in fact, to increase the photovoltage of the cell.[15] This trend motivates our investigation into the utilization of the good transport properties of PbSe nanoparticles without sacrificing open circuit voltage through the use of ultra-small quantum dots with larger bandgaps.

Results and Discussion

We describe here a new synthesis scheme producing strongly confined PbSe quantum dots with a diameter as small as 1 nm, and the effects of nanocrystal size on the photovoltaic performance of simple Schottky-type devices. In this study, we found that by varying the nanocrystal size, we can significantly increase the V_{OC} from 480 mV to 600 mV, which is the highest reported for a PbSe Schottky device to the best of our knowledge. The best device had a power conversion efficiency of 4.57% with AM1.5 illumination, which we achieved using PbSe quantum dots with a bandgap of ~1.6 eV (~2.3 nm diameter). While increasing the bandgap of the QDs has increased V_{OC}, it will eventually start to reduce J_{SC} due to lost absorption in the IR portion of the solar

4

spectrum. Thus, a fundamental tradeoff exists in finding the ideal PbSe QD size for optimal solar cell performance, but these effects have not yet been systematically investigated. Specifically, exploring the photovoltaic properties of ultra-small PbSe dots (< 3 nm in diameter) may reveal a simple way to increase the efficiency of nanocrystal solar cells without requiring more complex device architectures.

We successfully obtained monodisperse, ultra-small PbSe quantum dots using a one-pot, hot injection synthesis, modified from previous methods.[16, 17] Classical nucleation theory predicts that an initial burst of nuclei occurs when the monomer concentration in solution reaches supersaturation. The subsequent growth of particles occurs as the remaining monomers diffuse to the newly formed nuclei.[18] Following this theory, the ultra-small size of the PbSe dots obtained with our synthetic method can be explained by the combination of three factors: (1) a highly reactive selenium precursor, (2) a lower concentration of oleic acid, and (3) a high concentration of lead monomer in solution during the growth phase. First, to nucleate small particles, a more reactive selenium precursor must be used to facilitate fast nucleation kinetics.[19][20] We chose the highly reactive bis(trimethylsilyl) selenide ($(TMS)_2Se$) so that nearly all the selenium is used during the nucleation phase.[16] Reducing the oleic acid concentration makes the produced lead oleate monomer more reactive, also leading to faster nucleation kinetics.[21]   The large excess of lead monomer maintains a high reactant concentration post nucleation, which keeps the reaction in a size-focusing regime due to the smaller critical particle size. During the nanocrystal growth stage, the low temperature and limited Se supply left in the reaction solution hinders further growth and therefore restricts the final size of PbSe dots.[16] Our larger PbSe dots were obtained by adjusting the growth temperature from

5

room temperature to 180° C, which gradually increased nanocrystal size. Higher growth temperatures increase the critical nucleation concentration, limiting the number of initially nucleated particles and increasing the amount of monomer present during the growth process.

Transmission electron microscope (TEM) images of PbSe quantum dots grown at different temperatures were taken using a FEI Tecnai G2 S-TWIN, and are shown in Figure 1 with corresponding size histograms. Size statistics were measured from TEM images using ImageJ software assuming spherical particles. Image contrast decreases with particle size making good images difficult to obtain for very small particles. As a result, particle size distributions may be more narrow than reported due to image processing effects during analysis.
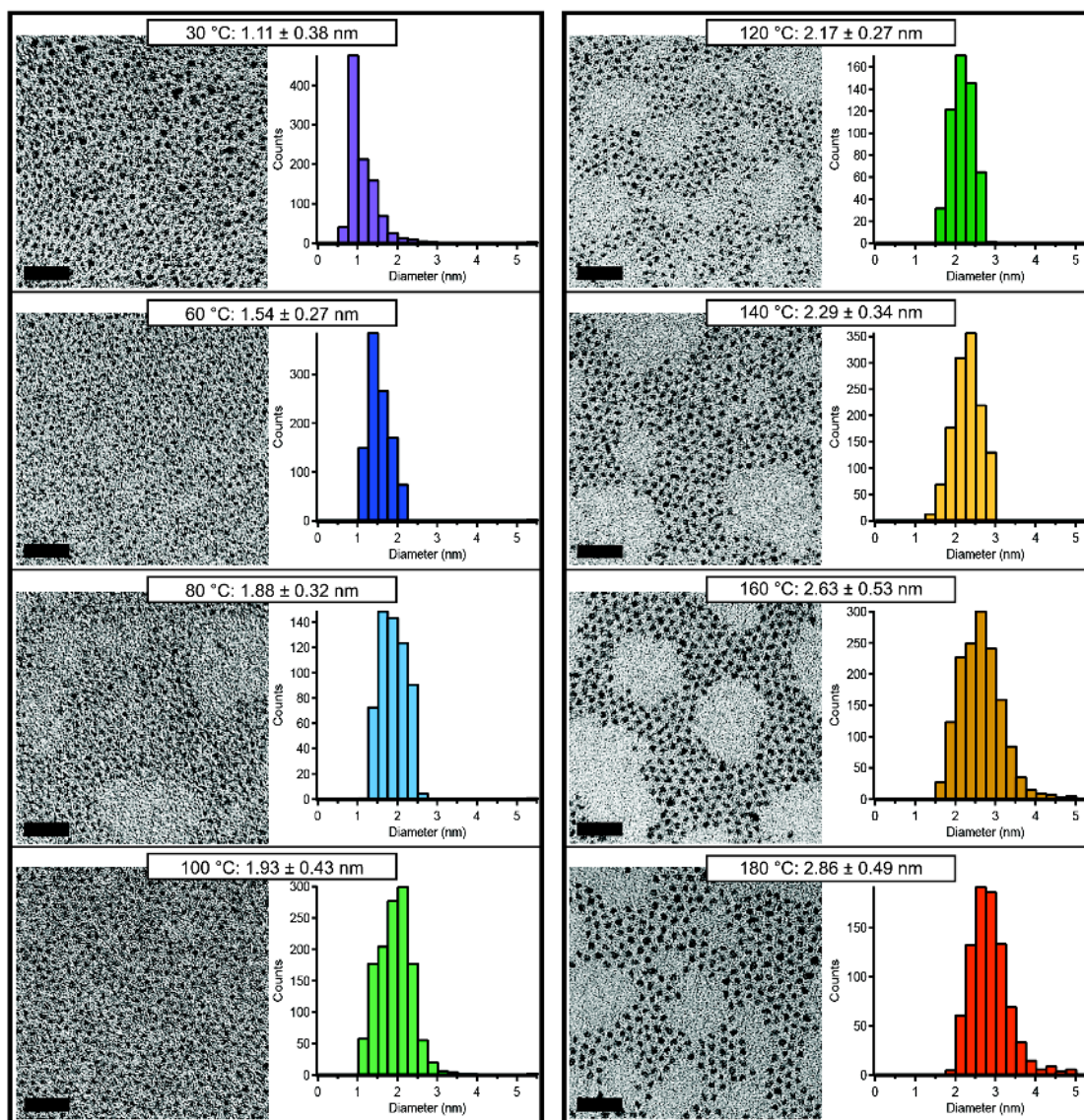
Figure 1. Transmission electron microscope (TEM) images of eight batches of ultra-small PbSe nanocrystals with diameters from 1~3 nm are shown. The growth temperature (indicated at the top of each panel) was controlled during the synthesis to yield different sized particles. Size analysis data are plotted in histograms for each sample, showing size distributions. All scale bars are 20 nm.

The absorption spectra of our PbSe quantum dots grown at different temperatures and a plot of the first exciton energy vs. growth temperature are shown in Figure 2a. The absorption peaks exhibit a linear dependence on the growth temperature, and the peak shapes indicate a narrow size dispersion of the quantum dots, especially at lower growth temperatures. As seen in Figure 2b, the average nanoparticle size is in good agreement with the trend extrapolated from equation 1 proposed by Quanqin Dai et al.:[22]

$$\hspace{10em} \boxed{} \hspace{10em} (1)$$

where d is the average nanoparticle diameter and λ is the wavelength of the first exciton absorption peak of the corresponding sample (both measured in nm). This agreement supports the accuracy of the size statistics obtained from TEM. Note that the smallest particles have a diameter of ~1 nm, which is roughly 1/50th of their exciton Bohr radius; to the best of our knowledge, this is the first time that PbSe quantum dots of this small size and narrow size dispersion have been reported. Under this extreme quantum confinement, their first exciton peak is blue shifted to 560 nm and they appear red when suspended in hexane (Figure 2c, inset), whereas larger particles typically appear brown.

Interestingly the photoluminescence (PL) spectrum for the smallest particles used in this study (d = 1.1 nm), shown in Figure 2c, exhibits a peak that is red-shifted approximately 170 nm from the absorption peak (733 nm and 560 nm, respectively). Previous optical studies of larger PbSe quantum dots have not noted such a large Stokes shift; nanoparticles with a diameter of 3-6 nm exhibited shifts of only 22-100 meV.[23-26] A theoretical study by Leitsmann et al. predicted a 170 meV red-shift for a PbSe QD 1.2 nm in diameter[27], significantly smaller than the ~560 meV shift present in our data.

However, Stokes shifts comparable to our results have been observed for strongly confined lead sulfide nanocrystals. PbS QDs (d = 1 nm) and nanorods (d = 1.7nm) have exhibited a red-shift of the PL peak by more than 500 meV[28] and 1.5 eV,[29] respectively.[29] One hypothesis from Fernée *et al*. to explain the large Stokes shift in lead chalcogenides is derived from excitonic fine structure splitting of the eightfold degenerate ground state, arising from inter-valley scattering.[30] While definitively identifying the origin of the large Stokes shift seen in our ultra-small particles is outside the scope of this work, further investigation is needed to understand how this optical behavior will affect the performance of solar cells made with these QDs. A more in-depth analysis of the size dependence of the Stokes shift in nanocrystals and the fine structure of the band edge exciton has been reported elsewhere.[26, 30-32]
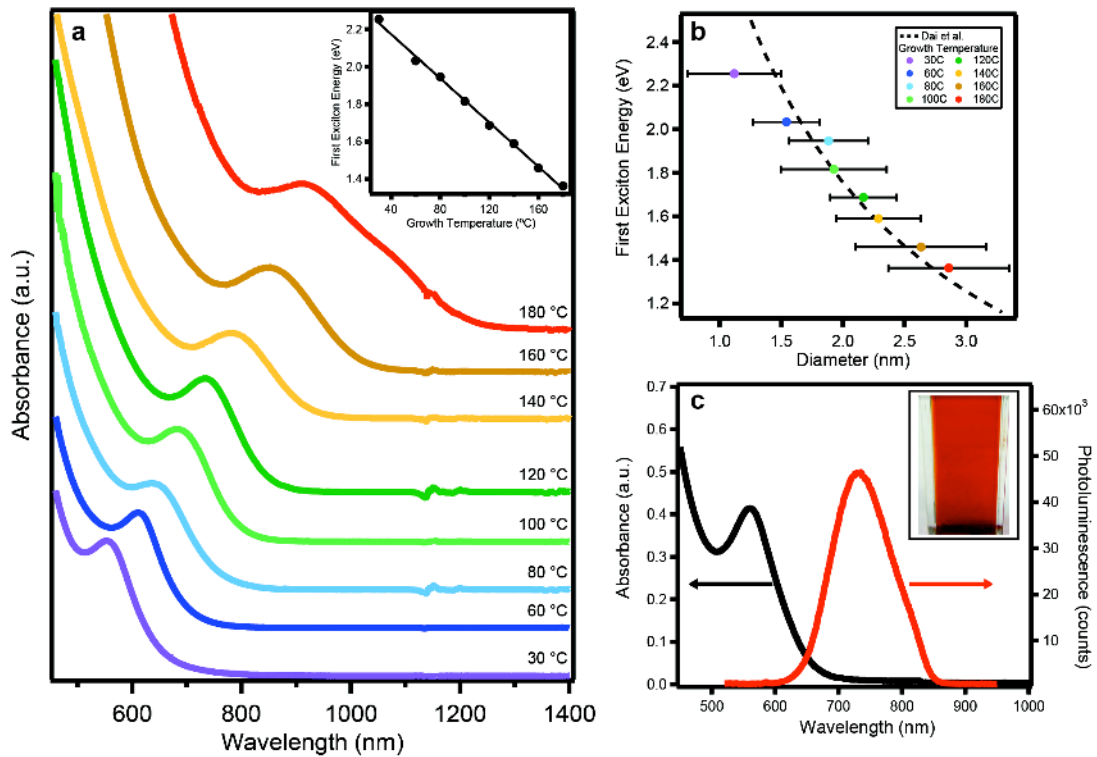
Figure 2. The absorbance of the ultra-small PbSe nanocrystals in solution, as-synthesized, is shown in (a). The first exciton peak blue shifts as the growth temperature (and thus the particle diameter) is decreased. By controlling the growth temperature during synthesis, we can produce particles with first exciton energies as large as 2.3 eV. The relationship between the first exciton energy and diameter of the particles is consistent with the model proposed by Dai *et al.*[22], shown as the dashed line in (b). The absorbance and photoluminescence of the smallest particles, grown at 30 °C, is shown in (c); the red color of the nanoparticle solution (c, inset) is due to their extreme quantum confinement. The slight shoulder on the red side of the PL peak may be explained by the asymmetric distribution of particle sizes (histogram in Figure 1), but the exact shape of the PL spectrum may be distorted by the loss in efficiency of the fluorimeter past ~850 nm.

To investigate the effects of quantum confinement on the photovoltaic performance, we adopted simple ITO/PEDOT/PbSe/Aluminum Schottky junction device structure using PbSe nanocrystals as the only photoactive material. The photovoltaic performance of solar cells fabricated using the eight different sizes of PbSe quantum dots is shown in Figure 3. Changing the size of the quantum dots involves a fundamental tradeoff between the open-circuit voltage and the short-circuit current, as we discussed previously. The open circuit voltage in Schottky solar cells has been shown to scale linearly with the bandgap[5], so devices made with smaller quantum dots should demonstrate a higher V_{OC}. As expected, the V_{OC} increases linearly from 0.48 V to 0.60 V for particles with bandgap

energy from 1.36 eV to 1.7 eV, similar to studies of larger dots. However, for dots with a bandgap larger than 1.7 eV (~2.3 nm diameter) the V_{OC} levels off and then starts to decrease. Since smaller dots have more surface area and require more interparticle hops per unit length, we hypothesize that charge recombination increases in the smaller particles. This also explains why the device fill factor (FF) has a clear decreasing trend for smaller dots since FF is directly related to recombination in the nanocrystal array film. Thus, the combination of increased recombination and reduced photocurrent outweighs the linear increase in V_{OC} for larger E_G. Despite this limitation, we obtained an open circuit voltage of 0.60 V which is the highest V_{OC} reported for PbSe quantum dot solar cells to our knowledge.

Figure 3 also clearly demonstrates that reducing the nanoparticle size leads to a monotonic decrease in the short-circuit current. In cells made with smaller PbSe nanocrystals, the increased bandgap results in reduced absorption in the red and infrared region of the solar spectrum, and thus a smaller J_{SC}. In addition to the reduced absorption, the loss of current may also be attributed to degraded transport through the film of smaller nanocrystals. Reduced mobilities have been seen for smaller PbSe dots, which may be a result of more interparticle hops needed for a photo-generated charge to traverse the cell, increased surface area, and/or increased depth of localized trap energies as the band edges move farther away with confinement.[33] An increase in trap densities and depths would also increase excess carrier recombination, reducing carrier lifetimes. These effects work together to reduce minority carrier diffusion lengths ($L_{Dif} = \sqrt{(kT/q)\mu\tau}$) and extraction probabilities, as any carriers generated outside the depletion region would have to diffuse to the region edge before recombining to be

11

efficiently extracted.[34]   As a result, for two devices of equivalent film thickness, the photovoltaic device utilizing smaller PbSe quantum dots generates less short-circuit current.
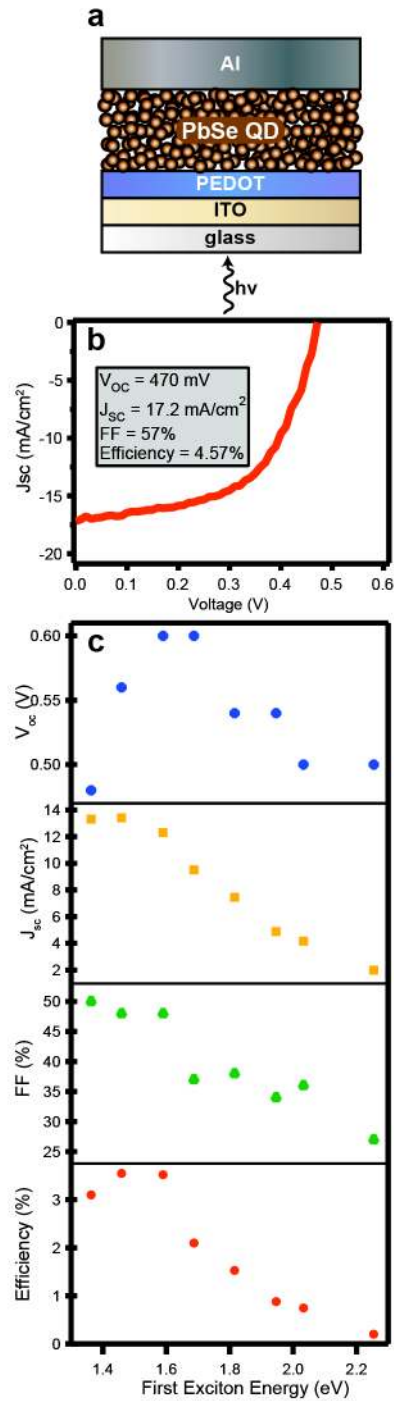
Figure 3. PbSe Schottky solar cells were fabricated as shown in (a). The *J-V* curve for the champion device (η = 4.57%), made with particles grown at 140 °C and exhibiting a first exciton absorption peak of 1.6 eV (measured in solution), is shown in (b). The effect of the nanocrystal size on the photovoltaic parameters (V_{OC}, J_{SC}, FF, Efficiency) is shown in (c). As expected, V_{OC} begins to increase as the first exciton energy increases for smaller particles, but then drops off rapidly for bandgaps above ~1.7 eV. This reduction in V_{OC} is most likely due to reduced absorption and poor transport through films of very small nanoparticles. The short circuit current decreases as a result of reduced absorption. The overall efficiency thus peaks around a bandgap of ~1.6 eV.

To better understand the photocurrent in our devices, we measured the external quantum efficiency (EQE) of PbSe solar cells made with different sized quantum dots (see Supplemental Information). Figure 4 shows the EQE for the most efficient QD size, with the first exciton peak (measured in solution) at 1.6 eV. In contrast to other reports,[5] the EQE curves do not coincide with the absorption curves of the colloidal nanocrystals (Figure 2a): the excitonic absorption features are noticeably absent in the EQE curves. We find that the shape of the EQE curve can be well-described by a simple optical model accounting for the coherent interference in thin films due to Fabry-Pérot cavity modes within the thickness of the PbSe.

The accuracy of the optical model depends first on measured optical constants for each of the materials in the device. Spectroscopic ellipsometry was used to measure the optical properties of the film of QDs grown at 140 ºC immediately after exposure to air. The

13

complex refractive index of the QD film was extracted after fitting to a Forouhi-Bloomer model,[35] which agreed closely with other complex refractive index data measured in the literature.[36] The optical properties of ITO were described using a Cauchy fit, and Al by a Lorentz-Drude fit to measurements from Palik.[37, 38] The modeled structure consists of a semi-infinite layer of glass, 150 nm of ITO, varying thickness of PbSe, and 100 nm of Al. The light is incident from within the glass layer. The calculations were done using the finite difference time-domain method (FDTD), and absorption in the PbSe layer was calculated directly from the electric field magnitude and refractive index according to P_{abs} = ½ ε'' $|\mathbf{E}|^2$. The incident source is a plane wave, and simulations were done at discrete wavelengths across the spectral range where these PbSe QDs are active (400 – 800 nm).

While this model is optical only and does not account for carrier collection, it is a reasonable method for calculation of the location of photocurrent peaks within the device, as seen from the agreement between the measured EQE curve and the simulated absorption profile in Figure 4a for a device thickness of 170 nm. Figure 4b illustrates the role of thickness of the PbSe layer in determining the shape of the EQE spectra. By varying the thickness in simulation from 140 nm to 300 nm, the absorption spectrum changes shape from one dominant peak around 550 nm to two dominant peaks.
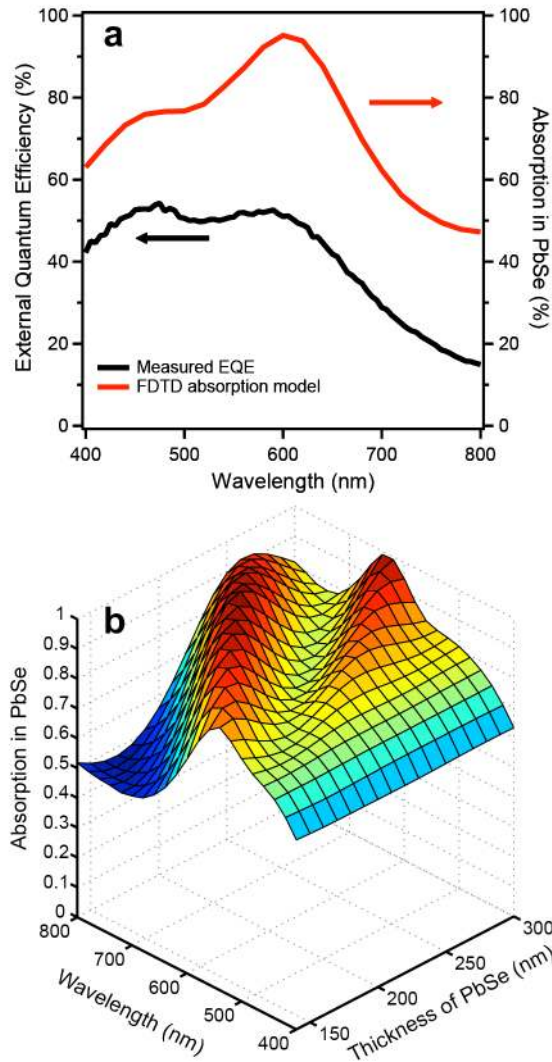
Figure 4. (a) The external quantum efficiency (EQE) spectrum of a solar cell made with PbSe nanocrystals (first exciton peak of 1.6 eV) is compared to the absorption in the PbSe film calculated with FDTD simulations for a film thickness matching that of the device. (b) Fabry-Pérot interference modes cause peaks in the absorption in the PbSe film; the wavelengths where the peaks occur depends on the thickness of the PbSe layer.

15

The drop off in power conversion efficiency of UV photons seen in Figure 4a could be explained by limited charge transport, or by optical losses in the ITO layer. Other groups have also observed this phenomenon and attributed the low EQE to the recombination of excitons before diffusion to the depleted region.[5] Higher energy blue photons are typically absorbed near the ITO interface in the quasi-neutral region, and the photogenerated charges have to diffuse to the depleted region for efficient separation. For films thick enough to absorb sufficient amount of light, these UV photons have a low probability of contributing to photocurrent.

Adjusting quantum dot size proved to be an effective approach to increase V_{OC} in PbSe Schottky devices, and ultimately to improve their overall power conversion efficiency. We observe that the best photovoltaic performance is achieved for devices using particles with the first exciton energy around 1.5~1.6 eV. Below this bandgap, higher photocurrent and fill factor can be achieved due to improved charge transport and enhanced absorbance, but the loss of V_{OC} due to decreased bandgap has a more pronounced impact and the overall device performance suffers. Reduced absorption and the degradation in transport through a film of small particles place an upper limit on the bandgap, but the latter could potentially be overcome with better passivation and increased electronic coupling. In order to achieve the best device performance, we must choose quantum dots with an appropriate size to optimize the tradeoff between J_{SC} and V_{OC}.

Additionally, the strongly confined PbSe nanocrystals synthesized for this study may enable further investigation of the effects of nanocrystal size on carrier multiplication (CM). Some recent reports[39,40] have concluded that CM is more efficient in nanocrystals

than in bulk solids, though the photophysics of CM in QDs is still a subject of debate.[15] Enhancing CM may provide a promising way forward for QD solar cells, but Nair *et al*. argue that the real benefit will come from the increased photovoltage of the extracted carriers resulting from quantum confinement of a material characterized by efficient CM in the bulk.[15] There has not yet been an experiment demonstrating an improvement in the overall power conversion efficiency of a solar cell as a result of CM; further experiments are needed to put the benefits of CM in perspective for photovoltaic device engineering.

In conclusion, we have developed a new synthesis to produce ultra-small PbSe quantum dots in the extreme quantum confinement regime, with diameters of 1~3 nm. We used a series of QDs with first exciton energies ranging from 1.3 ~ 2.3 eV to produce solar cells with different bandgaps. We observed that the open circuit voltage initially increases with bandgap, but the effect is diminished sooner than expected. Further investigations to identify the losses in the open circuit voltage and mitigate their effects are underway.

Methods

Nanocrystal synthesis. Lead oxide (PbO, 99.999%), oleic acid (OA, tech. grade, 90%), and 1-octadecene (ODE, 90%), anhydrous were purchased from Aldrich and used as received. Bis(trimethylsilyl) selenide (($TMS)_2Se$) was acquired from Gelest Inc. Nanocrystal synthesis was performed under argon atmosphere using standard air-free Schlenk line techniques. A solution of 223 mg PbO (1 mmol), 0.7 g oleic acid (2.5 mmol), and 10 g ODE was degassed at 100 °C in a 50 mL three-neck flask for an hour under vacuum. The solution was then heated for an additional hour to 150 °C under

argon. Before injection of the selenium precursor, the solution temperature was adjusted according to the desired nanocrystal size (see Table S1 of Supporting Information). When the temperature stabilized, 62 μL (TMS)$_2$Se (0.25 mmol) in 4 mL ODE was rapidly injected into the hot solution. Use caution and proper ventilation during this step, as toxic hydrogen selenide gas is also produced. We controlled the nanocrystal size and monodispersity by adjusting the injection temperature (30 °C to 180 °C) and the growth time (60 seconds to 30 minutes). Once complete, the reaction was rapidly quenched by injecting 10 mL of anhydrous hexane and submerging the flask in a room-temperature water bath. The nanocrystals were purified by precipitation twice in hexane/isopropanol and once in hexane/acetone and stored in hexane in an argon-filled glovebox.

Device fabrication. Patterned ITO-coated glass slides were acquired from Kintec (15 ohms/sq, ITO thickness ~150 nm). The substrates were cleaned by sonication in detergent, acetone, and isopropanol for 10 minutes in sequence, and then plasma cleaned for 5 minutes to remove any organic residue. A PEDOT (Baytron PH) film (~40 nm) was then spin-coated on top of the ITO surface to smooth it, and dried at 140 °C for 10 minutes. The PbSe nanocrystal film was deposited by multilayer spin-coating using a solution of quantum dots (60 mg/ml) dispersed in a 4:1 mixture of octane:hexane inside a glovebox. The slower-drying octane enables smoother nanoparticle layers, while the addition of hexane improves the wetting of the solution to the substrate. After each layer was deposited, the substrate was dipped briefly in a 0.001M 1,3-benzenedithiol (BDT, >98%) solution in acetonitrile to replace the oleic acid ligands with BDT. The BDT increases the coupling between particles allowing for better transport through the film, and allows deposition of additional nanocrystal layers due to the insolubility of the BDT-

18

coated particles in the octane:hexane solution.[8]   Following the ligand exchange, the device was rinsed with toluene while spinning to remove excess BDT and ligands. Aluminum contacts with a thickness of 100 nm were deposited by thermal evaporation at a rate of 0.1 nm/s for the first 10 nm and 0.3 nm/s for the remaining 90 nm at a pressure of $1x10^{-6}$ Torr.

Electrical characterization. Three devices were made for each batch of nanocrystals with eight working pixels on each device (active area of 4 mm^2). AM1.5G illumination from a Spectra Physics Oriel 300 W Solar Simulator was directed through a quartz window into an air-free glovebox, where the photovoltaic response of the devices was measured with a Keithley 236 source meter. The integrated intensity was set to 100 mW/cm^2 using a thermopile radiant power meter (Spectra Physics Oriel, model 70260) with fused silica window, and verified with a NREL calibrated Hamamatsu S1787-04 diode.

Supporting Information Available. Additional details of nanocrystal synthesis. Effect of thiol treatment on photoluminescence.   External quantum efficiency measurements.   This material is available free of charge *via* the Internet at http://pubs.acs.org.

Acknowledgments

References and Notes

1. Tang, J; Sargent, EH, Infrared Colloidal Quantum Dots for Photovoltaics: Fundamentals and Recent Progress. *Adv. Mater.* **2010,** *23*, 12-29.
2. Wise, F, Lead Salt Quantum Dots: The Limit of Strong Quantum Confinement. *Acc. Chem. Res.* **2000,** *33*, 773-780.
3. Kang, I; Wise, FW, Electronic Structure and Optical Properties of Pbs and Pbse Quantum Dots. *Journal of the Optical Society of America B* **1997,** *14*, 1632-1646.
4. Murray, CB; Sun, S; Gaschler, W; Doyle, H; Betley, TA; Kagan, CR, Colloidal Synthesis of Nanocrystals and Nanocrystal Superlattices. *IBM J. Res. Dev.* **2001,** *45*, 47-56.
5. Luther, JM; Law, M; Beard, MC; Song, Q; Reese, MO; Ellingson, RJ; Nozik, AJ, Schottky Solar Cells Based on Colloidal Nanocrystal Films. *Nano Lett.* **2008,** *8*, 3488-3492.
6. Johnston, KW; Pattantyus-Abraham, AG; Clifford, JP; Myrskog, SH; Macneil, DD; Levina, L; Sargent, EH, Schottky-Quantum Dot Photovoltaics for Efficient Infrared Power Conversion. *Appl. Phys. Lett.* **2008,** *92*, 151115.
7. Sun, B; Findikoglu, AT; Sykora, M; Werder, DJ; Klimov, VI, Hybrid Photovoltaics Based on Semiconductor Nanocrystals and Amorphous Silicon. *Nano Lett.* **2009,** *9*, 1235-1241.
8. Luther, J; Law, M; Song, Q; Perkins, C; Beard, M; Nozik, A, Structural, Optical, and Electrical Properties of Self-Assembled Films of Pbse Nanocrystals Treated with 1, 2-Ethanedithiol. *ACS Nano* **2008,** *2*, 271-280.
9. Tang, J; Brzozowski, L; Barkhouse, D; Wang, X; Debnath, R; Wolowiec, R; Palmiano, E; Levina, L; Pattantyus-Abraham, A; Jamakosmanovic, D*, et al.*, Quantum Dot Photovoltaics in the Extreme Quantum Confinement Regime: The Surface-Chemical Origins of Exceptional Air-and Light-Stability. *ACS Nano* **2010,** *4*, 869-878.
10. Pattantyus-Abraham, A; Kramer, I; Barkhouse, A; Wang, X; Konstantatos, G; Debnath, R; Levina, L; Raabe, I; Nazeeruddin, M; Grätzel, M*, et al.*, Depleted-Heterojunction Colloidal Quantum Dot Solar Cells. *ACS Nano* **2010,** *4*, 3374-3380.
11. Luther, J; Gao, J; Lloyd, M; Semonin, O; Beard, M; Nozik, A, Stability Assessment on a 3% Bilayer Pbs/Zno Quantum Dot Heterojunction Solar Cell. *Adv. Mater.* **2010,** *22*, 3704-3707.
12. Zarghami, MH; Liu, Y; Gibbs, M; Gebremichael, E; Webster, C; Law, M, P-Type Pbse and Pbs Quantum Dot Solids Prepared with Short-Chain Acids and Diacids. *ACS Nano* **2010,** *4*, 2475-2485.
13. Ma, W; Luther, JM; Zheng, H; Wu, Y; Alivisatos, AP, Photovoltaic Devices Employing Ternary Pbs X Se1-X Nanocrystals. *Nano Lett.* **2009,** *9*, 1699-1703.
14. Choi, JJ; Lim, YF; Santiago-Berrios, MB; Oh, M; Hyun, BR; Sung, LF; Bartnik, AC; Goedhart, A; Malliaras, GG; Abruna, HD*, et al.*, Pbse Nanocrystal Excitonic Solar Cells. *Nano Lett.* **2009,** *9*, 3749-3755.
15. Nair, G; Chang, L-Y; Geyer, SM; Bawendi, MG, Perspective on the Prospects of a Carrier Multiplication Nanocrystal Solar Cell. *Nano Lett.* **2011,** *11*, 2145-2151.
16. Hines, MA; Scholes, GD, Colloidal Pbs Nanocrystals with Size-Tunable near-Infrared Emission: Observation of Post-Synthesis Self-Narrowing of the Particle Size Distribution. *Adv. Mater.* **2003,** *15*, 1844-1849.
17. Evans, C; Guo, L; Peterson, J; Maccagnano-Zacher, S; Krauss, T, Ultrabright Pbse Magic-Sized Clusters. *Nano Lett.* **2008,** *8*, 2896-2899.
18. Peng, X; Wickham, J; Alivisatos, A, Kinetics of Ii-Vi and Iii-V Colloidal Semiconductor Nanocrystal Growth:"Focusing" of Size Distributions. *JACS* **1998,** *120*, 5343-5344.

19. An alternative approach would be to separate the nucleation and growth phases by employing an intermediate species, as shown by Kovalenko et al. to achieve PbSe quantum dots as small as 3.9 nm in diameter.

20. Kovalenko, MV; Talapin, DV; Loi, MA; Cordella, F; Hesser, G; Bodnarchuk, MI; Heiss, W, Quasi−Seeded Growth of Ligand−Tailored Pbse Nanocrystals through Cation−Exchange−Mediated Nucleation. *Angew. Chem. Int. Ed.* **2008,** *47*, 3029-3033.

21. Yu, W; Peng, X, Formation of High−Quality Cds and Other Ii–Vi Semiconductor Nanocrystals in Noncoordinating Solvents: Tunable Reactivity of Monomers. *Angew. Chem.* **2002,** *114*, 2474-2477.

22. Dai, Q; Wang, Y; Li, X; Zhang, Y; Pellegrino, DJ; Zhao, M; Zou, B; Seo, JT; Wang, Y; Yu, WW, Size-Dependent Composition and Molar Extinction Coefficient of Pbse Semiconductor Nanocrystals. *ACS Nano* **2009,** *3*, 1518-1524.

23. Du, H; Chen, C; Krishnan, R; Krauss, T; Harbold, J; Wise, F; Thomas, M; Silcox, J, Optical Properties of Colloidal Pbse Nanocrystals. *Nano Lett.* **2002,** *2*, 1321-1324.

24. Yu, W; Falkner, J; Shih, B; Colvin, V, Preparation and Characterization of Monodisperse Pbse Semiconductor Nanocrystals in a Noncoordinating Solvent. *Chem. Mater.* **2004,** *16*, 3318-3322.

25. Wehrenberg, B; Wang, C; Guyot-Sionnest, P, Interband and Intraband Optical Studies of Pbse Colloidal Quantum Dots. *J. Phys. Chem. B* **2002,** *106*, 10634-10640.

26. Lifshitz, E; Brumer, M; Kigel, A; Sashchiuk, A; Bashouti, M; Sirota, M; Galun, E; Burshtein, Z; Le Quang, A; Ledoux-Rak, I, Air-Stable Pbse/Pbs and Pbse/Pbsexs1-X Core− Shell Nanocrystal Quantum Dots and Their Applications†. *J. Phys. Chem. B* **2006,** *110*, 25356-25365.

27. Leitsmann, R; Bechstedt, F, Characteristic Energies and Shifts in Optical Spectra of Colloidal Iv− Vi Semiconductor Nanocrystals. *ACS Nano* **2009,** *3*, 3505-3512.

28. Warner, JH; Thomsen, E; Watt, AR; Heckenberg, NR; Rubinsztein-Dunlop, H, Time-Resolved Photoluminescence Spectroscopy of Ligand-Capped Pbs Nanocrystals. *Nanotechnology* **2005,** *16*, 175-179.

29. Acharya, S; Gautam, UK; Sasaki, T; Bando, Y; Golan, Y; Ariga, K, Ultra Narrow Pbs Nanorods with Intense Fluorescence. *JACS* **2008,** *130*, 4594-4595.

30. FernÈe, MJ; Thomsen, E; Jensen, P; Rubinsztein-Dunlop, H, Highly Efficient Luminescence from a Hybrid State Found in Strongly Quantum Confined Pbs Nanocrystals. *Nanotechnology* **2006,** *17*, 956-962.

31. Efros, AL; Rosen, M, The Electronic Structure of Semiconductor Nanocrystals. *Annu. Rev. Mater. Sci.* **2000,** *30*, 475-521.

32. An, J; Franceschetti, A; Zunger, A, The Excitonic Exchange Splitting and Radiative Lifetime in Pbse Quantum Dots. *Nano Lett.* **2007,** *7*, 2129-2135.

33. Liu, Y; Gibbs, M; Puthussery, J; Gaik, S; Ihly, R; Hillhouse, HW; Law, M, Dependence of Carrier Mobility on Nanocrystal Size and Ligand Length in Pbse Nanocrystal Solids. *Nano Lett.* **2010,** *10*, 1960-1969.

34. Johnston, KW; Pattantyus-Abraham, AG; Clifford, JP; Myrskog, SH; Hoogland, S; Shukla, H; Klem, EJD; Levina, L; Sargent, EH, Efficient Schottky-Quantum-Dot Photovoltaics: The Roles of Depletion, Drift, and Diffusion. *Appl. Phys. Lett.* **2008,** *92*, 122111.

35. Forouhi, A; Bloomer, I, Optical Dispersion Relations for Amorphous Semiconductors and Amorphous Dielectrics. *Physical Review B* **1986,** *34*, 7018-7026.

36. Law, M; Beard, MC; Choi, S; Luther, JM; Hanna, MC; Nozik, AJ, Determining the Internal Quantum Efficiency of Pbse Nanocrystal Solar Cells with the Aid of an Optical Model. *Nano Lett.* **2008,** *8*, 3904-3910.

37. Palik, ED, *Handbook of Optical Constants*. 1984; Vol. 1, p 1297-1297.

38. Rakic, AD; Djurišic, AB; Elazar, JM; Majewski, ML, Optical Properties of Metallic Films for Vertical-Cavity Optoelectronic Devices. *Appl. Opt.* **1998,** *37*, 5271-5283.

39.   Beard, MC; Midgett, AG; Hanna, MC; Luther, JM; Hughes, BK; Nozik, AJ, Comparing Multiple Exciton Generation in Quantum Dots to Impact Ionization in Bulk Semiconductors: Implications for Enhancement of Solar Energy Conversion. *Nano Lett.* **2010,** *10,* 3019-3027.

40. Nootz, G; Padilha, LA; Levina, L; Sukhovatkin, V; Webster, S; Brzozowski, L; Sargent, EH; Hagan, DJ; Van Stryland, EW, Size Dependence of Carrier Dynamics and Carrier Multiplication in Pbs Quantum Dots. *Physical Review B* **2011,** *83,* 155302.

DISCLAIMER

DE-AC02-05CH11231